Analyst

PAPER

View Article Online
View Journal | View Issue

Cite this: *Analyst*, 2014, **139**, 1692

Facile synthesis of water-soluble and biocompatible fluorescent nitrogen-doped carbon dots for cell imaging†

Weiping Wang, Ya-Chun Lu, Hong Huang, Jiu-Ju Feng,* Jian-Rong Chen and Ai-Jun Wang*

Received 9th November 2013
Accepted 8th January 2014

DOI: 10.1039/c3an02098c

www.rsc.org/analyst

A simple, facile and green hydrothermal method was developed in the synthesis of water-soluble nitrogen-doped carbon dots (N-CDs) from streptomycin. The as-prepared N-CDs displayed bright blue fluorescence under the irradiation of UV light, together with a high quantum yield of 7.6% and good biocompatibility as demonstrated by the cell viability assay. Thus, the N-CDs can be used as fluorescent probes for cell imaging, which have potential applications in bioimaging and related fields. This strategy opens a new way for the preparation of fluorescent carbon nanomaterials using small molecules as carbon sources.

Introduction

Considerable attention has been paid to fluorescent carbon nanomaterials over past several years, owing to their unique physical properties and numerous promising applications in nanobiotechnology. Carbon dots (CDs), as a new member of the carboxylated carbonaceous materials family, have attracted tremendous interest since their discovery.[1] Their unique properties are largely attributed to their large surface area, good biocompatibility, and chemical inertness, as well as their unique electronic, optical and thermal characteristics. The CDs have promising potential applications in biological labeling,[2] bioimaging,[3–6] biosensing,[7] and optoelectronic devices.[8,9] Their advantages over other types of semiconductor quantum dots are ascribed to their good biocompatibility and low toxicity.[10–12] Thus, many methods have been developed, which are mainly classified into two types (*i.e.* top-down and bottom-up synthesis).[9,13] Specifically, the 'top-down' approach is a method of breaking bulk material into small pieces by acid oxidation, electrochemical oxidation, and thermal decomposition.[14–17] Alternatively, 'bottom-up' methods include wet-chemical, solvothermal, and microwave-assisted methods, in which the CDs are prepared from molecular precursors under specific reaction conditions.[9,18–20]

To improve the solubility and fluorescent properties of the CDs, especially the intrinsic low emission efficiency, several strategies have been designed to extend their applications in biosensing and bioimaging, such as surface passivation and doping with inorganic salts.[20–23] For instance, doping with nitrogen is widely used, because the nitrogen atom has a comparable atomic size and five valence electrons to bind carbon atoms.[24] Such functionalization can improve the properties of the CDs, as well as extending their potential and/or practical applications.[20,25] Zhang *et al.* prepared nitrogen-doped CDs (N-CDs) from dried monkey grass for the detection of iodide.[26] Wu and co-workers fabricated N-CDs from Bombyx mori silk and used them as a fluorescent probe in bioimaging.[25] Xu's group synthesized multicolor N-CDs using L-alanine, L-histidine, and L-arginine as precursors, and applied them to the living cell system.[27] However, complex procedures and strong acid treatment are usually involved.[28–30]

In this work, a simple and facile method was developed for the one-step hydrothermal synthesis of fluorescent N-CDs from streptomycin. Their emission properties, quantum yield, stability, solubility and toxicity were investigated in detail.

Experimental

Chemicals

Streptomycin was purchased from Aladdin Ltd. (Shanghai, China). All the other chemicals were of analytical grade and used as received. Twice-distilled water was used for preparation of all aqueous solutions in the whole experiments.

Preparation of the N-CDs

The N-CDs were prepared by hydrothermal treatment of streptomycin (Fig. 1). Typically, 0.1 g streptomycin was dissolved in 35 mL of water under stirring. The solution was transferred to a 50 mL Teflon-lined autoclave, heated at 200 °C for 12 h, and cooled to room temperature naturally. Next, the aqueous solution was centrifuged at 12000 rpm for

College of Chemistry and Life Science, College of Geography and Environmental Science, Zhejiang Normal University, Jinhua 321004, China. E-mail: jjfeng@zjnu.cn; ajwangnju@gmail.com; Fax: +86-579-82282269; Tel: +86-579-82282269

† Electronic supplementary information (ESI) available. See DOI: 10.1039/c3an02098c

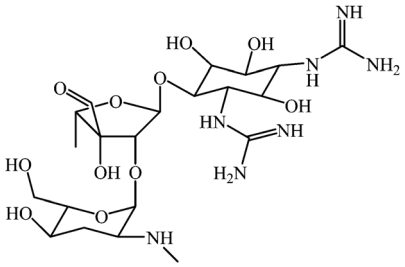

Fig. 1 Chemical structure of streptomycin.

20 min to discard the non-fluorescent deposit, while the N-CDs suspension was kept for further characterization.

Instruments

UV-vis absorption spectra of the samples were recorded using a Lambda 950 UV-vis spectrophotometer (Perkin-Elmer, USA). Fluorescence spectroscopy measurements were conducted using an LS-45 fluorescence spectrophotometer (Perkin-Elmer, UK). Fluorescence lifetime experiments were performed on an Edinburgh FLS 920 photo-counting system. X-ray diffraction (XRD) analysis was carried out using a Philips PW3040/60 automatic powder diffractometer using Cu Kα radiation. Fourier transform infrared spectroscopy (FT-IR) experiments were conducted on a Nicolet 670 FT-IR spectrometer in the form of KBr pellets. Zeta potentials were measured using a Malvern Zetasizer Nano ZS dynamic light scattering system. The fluorescence images were acquired using a Leica laser confocal fluorescence microscope (TCS SP5).

Cell imaging and toxicity assay

The cytotoxicity of the N-CDs to human epithelial carcinoma (Hela) cells was evaluated by a standard methylthiazolydiphenyltetrazolium bromide (MTT) assay. Hela cells were seeded in 96-well U-bottom plates at a density of approx 5×10^4 to 1×10^5 cells per mL (90 μL per well) that were initially cultured for 12 h in an incubator (37 °C, 5% CO_2), followed by the addition of the N-CDs suspension with different concentrations. After another 24 h of being cultured with the N-CDs, 20 μL of the MTT solution (normal saline or 1 mg mL^{-1} phosphate buffer solution) was added to each sample and incubated at 37 °C for 4 h. The culture media were discarded, followed by the addition of 150 μL of dimethyl sulfoxide (DMSO) to dissolve the formazan under shaking for more than 15 min. The corresponding spectra were recorded with a microplate reader at 570 nm. The cell viability rate (VR) was calculated based on the following equation:

$$\mathrm{VR}\ (\%) = A/A_0 \times 100\%$$

where A is the absorbance of the experimental group (the cells that were treated with the N-CDs suspensions) and A_0 is the absorbance of the control group.

Results and discussion

Fig. 2A shows the typical UV-vis absorption spectrum of the as-prepared N-CDs. Clearly, a strong peak is detected at 275 nm, which is attributed to the π–π* transition of the C=O bond,[25,31] revealing the typical absorption of the aromatic π orbitals, which is consistent with that of polycyclic aromatic hydrocarbons.[32] The N-CDs suspension displays the light yellow color (inset 1 in Fig. 2A), which exhibits bright blue fluorescence under UV light at an excitation of 365 nm (inset 2 in Fig. 2A). Furthermore, the sample shows the maximum emission peak centered at 410 nm, with a full width at half maximum (FWHM) of 94 nm, which is similar to that of the carbon particles obtained from strawberry juice,[33] but different from that prepared with glycine.[34] Meanwhile, with the variation of the excitation wavelength from 333 to 500 nm, the N-CDs emit at longer wavelength (Fig. 2B), displaying tunable emission properties. Therefore, the N-CDs exhibit an excitation-dependent emission, which is an intrinsic property of the carbon particles, as demonstrated previously in extensive reports.[23,35–37]

The fluorescence quantum yield is about 7.6%, using quinine sulfate (54% in 0.1 mol L^{-1} H_2SO_4, $\lambda_{ex} = 333$ nm) as a reference. This value is similar to the carbon nanoparticles reported previously,[4,14,38] but larger than those prepared from ascorbic acid,[29] glucose and 4,7,10-trioxa-1,13-tridecanediamine.[39] This is ascribed to the surface passivation of the CDs in the present work. The fluorescence lifetime is measured to be 7.42 ns, with excitation and emission wavelengths of 333 and 410 nm, respectively (see Fig. S1, Supporting Information†). This value is higher than those of the carbon nanoparticles reported before.[4,25,40]

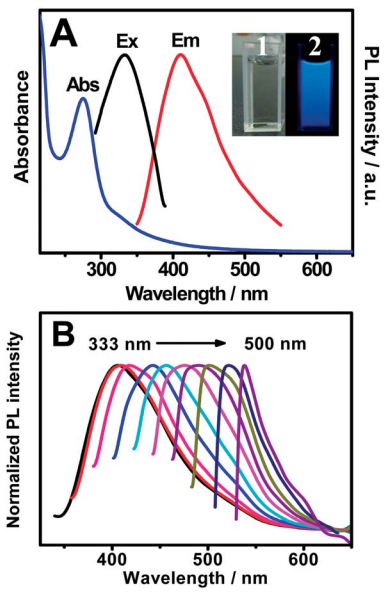

Fig. 2 (A) UV-vis absorption spectrum (blue), photoluminescence excitation (black), and emission (red) spectra of the N-CDs in aqueous solutions. (B) The corresponding emission spectra by varying the excitation wavelengths from 333 to 500 nm with 20 nm increment. Insets show the corresponding photographs under visible light (1) and UV light (2), respectively.

Representative TEM image clearly reveals that the N-CDs are nearly spherical with a diameter of 2.97 nm (Fig. 3B). Moreover, the high-resolution TEM (HRTEM) image (inset in Fig. 3A) displays the clear lattice fringes with an interfringe distance of 0.202 nm, which is assigned to the (102) planes of graphitic (sp^2) carbon.[41] This observation is similar to that fabricated from graphite powder,[42] but different from that of the carbon nanoparticles synthesized with activated carbon.[43]

Impressively, the N-CDs show a diffraction peak located at 22.6° in the XRD spectrum (Fig. 4A), suggesting that the interlayer spacing of the (002) diffraction peak is 0.41 nm, similar to that of the carbon nanoparticles prepared from citric acid with branched polyethylenimine,[44] but larger than that of graphite (0.34 nm), possibly owing to the existence of oxygen-containing functional groups.[40]

The functional groups of the N-CDs were characterized by FT-IR spectroscopy (Fig. 4B). There is a broad peak at around 3420 cm^{-1}, corresponding to the O–H stretching vibration, indicating the presence of abundant hydroxyl groups. The peak at 1640 cm^{-1} is attributed to the C=O stretching mode. And the peaks at 1400 cm^{-1} and 1100 cm^{-1} come from the C–O–C groups.[16,29,32,41,45] These observations demonstrate the coexistence of hydroxyl and carboxylic groups on the surface of the N-CDs, as also supported by zeta potential experiments with a value of −29.4 mV.[14,20]

The surface composition and oxidation states of the N-CDs were examined by XPS measurements. In the survey XPS spectrum, the peaks at 286.1 eV, 402.1 eV, and 532.1 eV (Fig. 5A) correspond to the elements of C_{1s}, N_{1s}, and O_{1s}, respectively. These results indicate that the N-CDs are composed of C, O, and N elements at the percentages of 60.26%, 26.73%, and 9.15%, respectively. The amount of N is smaller than that fabricated from cocoon silk,[20] but higher than those prepared from strawberry juice[33] and grass.[46] It indicates that streptomycin can be used for surface passivation of the CDs. Specifically, the deconvolution of the C_{1s} peak (Fig. 5B) indicates the existence of sp^2 C=C (284.8 eV), C–O (286.2 eV), and C=O (287.9 eV) groups. There are two peaks observed at 530.7 eV and 532.0 eV in the O_{1s} spectrum (Fig. 5C), which are assigned to the C=O and C–OH/C–O–C groups, respectively. The N_{1s} spectrum (Fig. 5D) has two peaks at 399.9 eV and 401.4 eV, which are attributed to the C–N–C and N–$(C)_3$ groups, respectively.

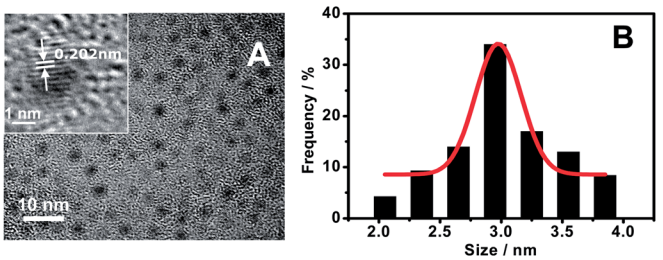

Fig. 3 TEM image (A) and the particle size distribution (B) of the N-CDs. Inset shows the high-magnification TEM image of a nitrogen-doped carbon dot.

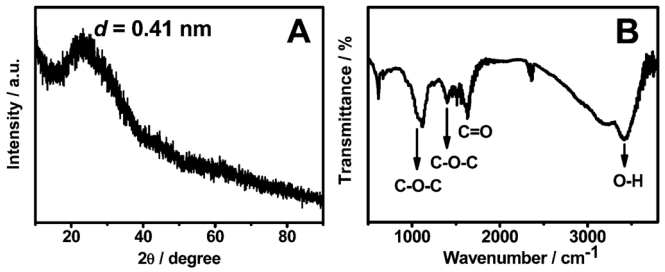

Fig. 4 XRD pattern (A) and FT-IR spectrum (B) of the N-CDs.

Herein, a series of control experiments were performed to examine the stability of the N-CDs. As shown in Fig. 6A, the fluorescence intensities are almost unchanged by varying the NaCl concentrations (up to 500 mM), revealing high stability of the N-CDs even under high ionic-strength conditions. Similarly, the fluorescence intensity is nearly constant after the sample has been treated with a 500 W Xe lamp for 6 h (Fig. 6C) or stored for three months (Fig. 6D), while other conditions were kept unchanged. Alternatively, the variation of the pH value from 3 to 10 has a slight effect on the fluorescence intensity (Fig. 6B), whereas the intensity drops down as the pH is increased up to 12. As a result, the N-CDs have good stability over the entire physiological pH range, enabling them to have a wide range of applications, unlike those obtained from polyethylenimine[47] and citric acid.[48] These results verify the improved stability of the N-CDs, possibly owing to the electrostatic repulsions between the negatively charged nanoparticles. Therefore, the N-CDs are particularly valuable for real applications in bio-labelling and bio-imaging.

To demonstrate the as-prepared N-CDs as fluorescent probes in cell imaging, the MTT assay was carried out using Hela cells as the model cell (Fig. 7). The N-CDs exhibit fairly low cytotoxicity with cells retaining a viability of 100% and 78% at the

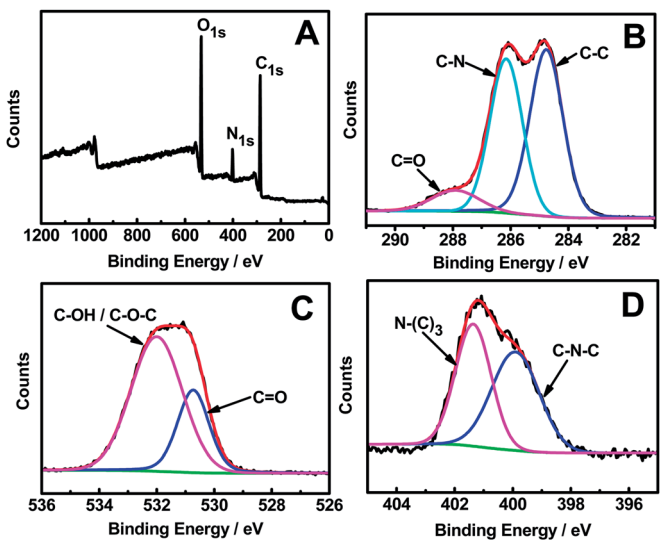

Fig. 5 XPS survey (A), and high-resolution C_{1s} (B), O_{1s} (C) and N_{1s} (D) spectra of the N-CDs.

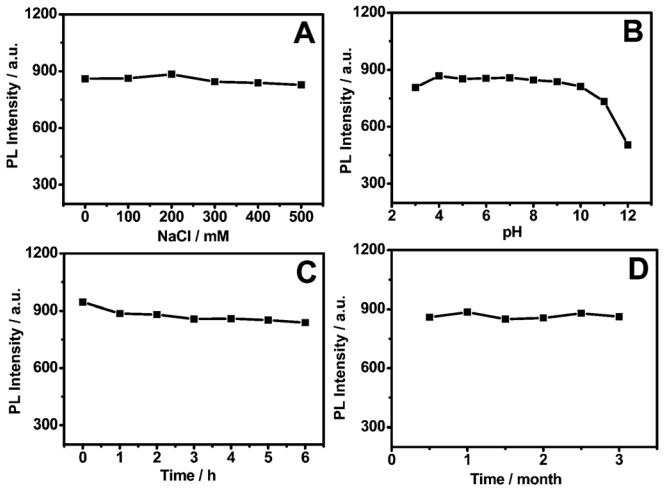

Fig. 6 Effects of NaCl concentration (A), pH value from 3 to 12 (B), time intervals of irradiation with a 500 W Xe lamp (C), and storage time (D) on the fluorescence intensity of the N-CDs.

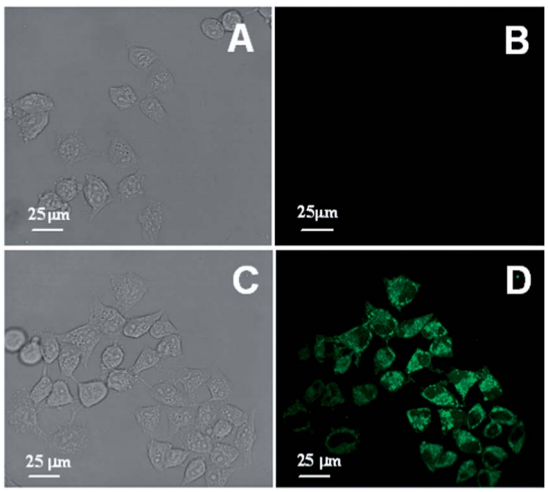

Fig. 8 Images of Hela cells in the absence (A, B) and presence (C, D) of the CDs obtained under bright field (A, C) and by excitation at 488 nm (B, D). The concentration of the CDs is 55 μg mL^{-1}.

concentration of 55 and 825 μg mL^{-1}, respectively, suggesting low cytotoxicity and good biocompatibility of the N-CDs, compared with those in the literature.[13,39,49]

Impressively, the N-CDs concentrations are much higher for the *in vitro* evaluation, compared with those required for potential applications such as the optical imaging of living cells.[50] Similarly, the exposure time under UV light is much longer than the routine use. This means that the N-CDs possess chemical inertness and almost no cytotoxicity, even in harsh environments.

Importantly, the uptake of the N-CDs and bioimaging experiments were also performed using a confocal fluorescence microscope *in vitro*. As illustrated in Fig. 8, the morphologies of the Hela cells are almost unchanged before (Fig. 8A) and after (Fig. 8C) incubation with the N-CDs, further confirming their good biocompatibility and low toxicity. The bright green areas inside the Hela cells are clearly observed by excitation at 488 nm (Fig. 8D), although it is hard to distinguish the fluorescent area under bright field conditions (Fig. 8B). These results suggest the good stability of the N-CDs. Notably, the fluorescent spots are observed only in the cytoplasm, whereas very weak fluorescence intensity is detected in the central region, indicating that the N-CDs are easy to penetrate into the cells but only into the cytoplasm. This observation is consistent with the previous studies on the interactions of living cells with nanomaterials,[2,51,52] in which genetic disruption does not occur.[50] All these results demonstrate the very good biocompatibility of the N-CDs, which can be used as an excellent optical probe for cell imaging.

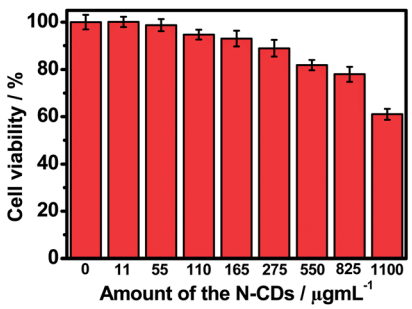

Fig. 7 Cell viability assays of the cells treated with different concentrations of the N-CDs.

Conclusion

In summary, a simple, facile, efficient and green method was developed for preparation of fluorescent N-CDs using streptomycin as the carbon source. The as-synthesized water-soluble N-CDs showed bright and stable blue fluorescence, which was closely dependent on the excitation wavelength. The N-CDs have tunable emission properties, excellent stability and low cytotoxicity. These advantages make the N-CDs a promising imaging agent in bioimaging, protein analysis and cell tracking. This strategy may open a new route for constructing other functional carbon nanomaterials as highly specific catalysts and drug-targeting carriers.

Acknowledgements

This work was financially supported by the NSFC (Nos. 21175118, 21275130, 21275131, 21305128 and 21345006), and Zhejiang province university young academic leaders of academic climbing project (No. pd2013055).

References

1 X. Xu, R. Ray, Y. Gu, H. J. Ploehn, L. Gearheart, K. Raker and W. A. Scrivens, *J. Am. Chem. Soc.*, 2004, **126**, 12736–12737.
2 M. Zhang, L. Bai, W. Shang, W. Xie, H. Ma, Y. Fu, D. Fang, H. Sun, L. Fan, M. Han, C. Liu and S. Yang, *J. Mater. Chem.*, 2012, **22**, 7461–7467.
3 S. Zhuo, M. Shao and S.-T. Lee, *ACS Nano*, 2012, **6**, 1059–1064.

4 J. Zhou, Z. Sheng, H. Han, M. Zou and C. Li, *Mater. Lett.*, 2012, **66**, 222–224.
5 C. Yu, X. Li, F. Zeng, F. Zheng and S. Wu, *Chem. Commun.*, 2013, **49**, 403–405.
6 P.-C. Hsu, P.-C. Chen, C.-M. Ou, H.-Y. Chang and H.-T. Chang, *J. Mater. Chem. B*, 2013, **1**, 1774–1781.
7 S. Zhu, Q. Meng, L. Wang, J. Zhang, Y. Song, H. Jin, K. Zhang, H. Sun, H. Wang and B. Yang, *Angew. Chem.*, 2013, **125**, 4045–4049.
8 C. Zhu, J. Zhai and S. Dong, *Chem. Commun.*, 2012, **48**, 9367–9369.
9 J. Shen, Y. Zhu, X. Yang and C. Li, *Chem. Commun.*, 2012, **48**, 3686–3699.
10 L. Zhou, Z. Li, Z. Liu, J. Ren and X. Qu, *Langmuir*, 2013, **29**, 6396–6403.
11 S.-T. Yang, L. Cao, P. G. Luo, F. Lu, X. Wang, H. Wang, M. J. Meziani, Y. Liu, G. Qi and Y.-P. Sun, *J. Am. Chem. Soc.*, 2009, **131**, 11308–11309.
12 X. Wang, K. Qu, B. Xu, J. Ren and X. Qu, *Nano Res.*, 2011, **4**, 908–920.
13 Z. Qian, J. Ma, X. Shan, L. Shao, J. Zhou, J. Chen and H. Feng, *RSC Adv.*, 2013, **3**, 14571–14579.
14 H. Yan, M. Tan, D. Zhang, F. Cheng, H. Wu, M. Fan, X. Ma and J. Wang, *Talanta*, 2013, **108**, 59–65.
15 H. Li, X. He, Z. Kang, H. Huang, Y. Liu, J. Liu, S. Lian, C. H. A. Tsang, X. Yang and S.-T. Lee, *Angew. Chem., Int. Ed.*, 2010, **49**, 4430–4434.
16 Y. Dong, H. Pang, S. Ren, C. Chen, Y. Chi and T. Yu, *Carbon*, 2013, **64**, 245–251.
17 Y. Dong, N. Zhou, X. Lin, J. Lin, Y. Chi and G. Chen, *Chem. Mater.*, 2010, **22**, 5895–5899.
18 Y. Yang, D. Wu, S. Han, P. Hu and R. Liu, *Chem. Commun.*, 2013, **49**, 4920–4922.
19 Y. N. Tan, J. Y. Lee and D. I. C. Wang, *J. Am. Chem. Soc.*, 2010, **132**, 5677–5686.
20 W. Li, Z. Zhang, B. Kong, S. Feng, J. Wang, L. Wang, J. Yang, F. Zhang, P. Wu and D. Zhao, *Angew. Chem., Int. Ed.*, 2013, **52**, 1–6.
21 F. L. Braghiroli, V. Fierro, M. T. Izquierdo, J. Parmentier, A. Pizzi and A. Celzard, *Carbon*, 2012, **50**, 5411–5420.
22 P. Wu and X.-P. Yan, *Chem. Soc. Rev.*, 2013, **42**, 5489–5521.
23 J. Shen, Y. Zhu, X. Yang, J. Zong, J. Zhang and C. Li, *New J. Chem.*, 2012, **36**, 97–101.
24 Y. Li, Y. Zhao, H. Cheng, Y. Hu, G. Shi, L. Dai and L. Qu, *J. Am. Chem. Soc.*, 2011, **134**, 15–18.
25 Z. L. Wu, P. Zhang, M. X. Gao, C. F. Liu, W. Wang, F. Leng and C. Z. Huang, *J. Mater. Chem. B*, 2013, **1**, 2868–2873.
26 H. Zhang, Y. Li, X. Liu, P. Liu, Y. Wang, T. An, H. Yang, D. Jing and H. Zhao, *Environ. Sci. Technol. Lett.*, 2014, **1**, 87–91.
27 Y. Xu, M. Wu, Y. Liu, X.-Z. Feng, X.-B. Yin, X.-W. He and Y.-K. Zhang, *Chem.–Eur. J.*, 2013, **19**, 2276–2283.
28 M. Tan, L. Zhang, R. Tang, X. Song, Y. Li, H. Wu, Y. Wang, G. Lv, W. Liu and X. Ma, *Talanta*, 2013, **115**, 950–956.
29 X. Jia, J. Li and E. Wang, *Nanoscale*, 2012, **4**, 5572–5575.
30 S. Liu, L. Wang, J. Tian, J. Zhai, Y. Luo, W. Lu and X. Sun, *RSC Adv.*, 2011, **1**, 951–953.
31 A. Sachdev, I. Matai, S. U. Kumar, B. Bhushan, P. Dubey and P. Gopinath, *RSC Adv.*, 2013, **3**, 16958–16961.
32 R. Liu, H. Li, W. Kong, J. Liu, Y. Liu, C. Tong, X. Zhang and Z. Kang, *Mater. Res. Bull.*, 2013, **48**, 2529–2534.
33 H. Huang, J.-J. Lv, D.-L. Zhou, N. Bao, Y. Xu, A.-J. Wang and J.-J. Feng, *RSC Adv.*, 2013, **3**, 21691–21696.
34 P.-C. Hsu and H.-T. Chang, *Chem. Commun.*, 2012, **48**, 3984–3986.
35 J. Zhou, Y. Yang and C.-Y. Zhang, *Chem. Commun.*, 2013, **49**, 8605–8607.
36 Y.-P. Sun, B. Zhou, Y. Lin, W. Wang, K. A. S. Fernando, P. Pathak, M. J. Meziani, B. A. Harruff, X. Wang, H. Wang, P. G. Luo, H. Yang, M. E. Kose, B. Chen, L. M. Veca and S.-Y. Xie, *J. Am. Chem. Soc.*, 2006, **128**, 7756–7757.
37 H. Peng and J. Travas-Sejdic, *Chem. Mater.*, 2009, **21**, 5563–5565.
38 J. Wei, J. Shen, X. Zhang, S. Guo, J. Pan, X. Hou, H. Zhang, L. Wang and B. Feng, *RSC Adv.*, 2013, **3**, 13119–13122.
39 Y. Song, W. Shi, W. Chen, X. Li and H. Ma, *J. Mater. Chem.*, 2012, **22**, 12568–12573.
40 J. Peng, W. Gao, B. K. Gupta, Z. Liu, R. Romero-Aburto, L. Ge, L. Song, L. B. Alemany, X. Zhan, G. Gao, S. A. Vithayathil, B. A. Kaipparettu, A. A. Marti, T. Hayashi, J.-J. Zhu and P. M. Ajayan, *Nano Lett.*, 2012, **12**, 844–849.
41 W. Lu, X. Qin, S. Liu, G. Chang, Y. Zhang, Y. Luo, A. M. Asiri, A. O. Al-Youbi and X. Sun, *Anal. Chem.*, 2012, **84**, 5351–5357.
42 S.-L. Hu, K.-Y. Niu, J. Sun, J. Yang, N.-Q. Zhao and X.-W. Du, *J. Mater. Chem.*, 2009, **19**, 484–488.
43 Y. Dong, C. Chen, J. Lin, N. Zhou, Y. Chi and G. Chen, *Carbon*, 2013, **56**, 12–17.
44 Y. Dong, R. Wang, H. Li, J. Shao, Y. Chi, X. Lin and G. Chen, *Carbon*, 2012, **50**, 2810–2815.
45 H. Zhu, X. Wang, Y. Li, Z. Wang, F. Yang and X. Yang, *Chem. Commun.*, 2009, 5118–5120.
46 S. Liu, J. Tian, L. Wang, Y. Zhang, X. Qin, Y. Luo, A. M. Asiri, A. O. Al-Youbi and X. Sun, *Adv. Mater.*, 2012, **24**, 2037–2041.
47 L. Shen, L. Zhang, M. Chen, X. Chen and J. Wang, *Carbon*, 2013, **55**, 343–349.
48 W. Shi, X. Li and H. Ma, *Angew. Chem.*, 2012, **124**, 6538–6541.
49 L. Shang, R. M. Dorlich, S. Brandholt, R. Schneider, V. Trouillet, M. Bruns, D. Gerthsen and G. U. Nienhaus, *Nanoscale*, 2011, **3**, 2009–2014.
50 F. Wang, Z. Xie, H. Zhang, C.-Y. Liu and Y.-G. Zhang, *Adv. Funct. Mater.*, 2011, **21**, 1027–1031.
51 X. Zhai, P. Zhang, C. Liu, T. Bai, W. Li, L. Dai and W. Liu, *Chem. Commun.*, 2012, **48**, 7955–7957.
52 Y. Xu, M. Wu, X.-Z. Feng, X.-B. Yin, X.-W. He and Y.-K. Zhang, *Chem.–Eur. J.*, 2013, **19**, 6282–6288.

